content of an image, and more particularly, to a method and apparatus for combining nonlinear functions of intensity of multiple images to form three dimensional patterns with spatial frequencies that are not present in any of the individual exposures and whose magnitudes are larger than $2/\lambda$, the limit of linear optical system response, in all three spatial directions.

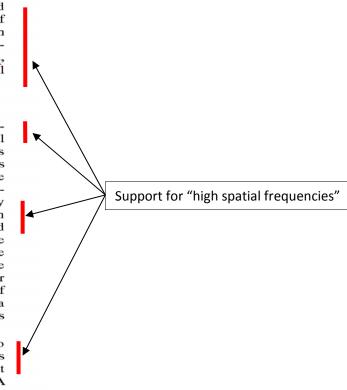
BACKGROUND OF THE INVENTION

The quality of an image is limited by the spatial frequencies within the image. In general, the maximum spatial frequency contained in an optically defined image is $\sim 2NA/\lambda$ where NA is the lens numerical aperture (the radius of the lens aperture divided by the distance from the exit face of the lens to the focal plane) and λ is the optical wavelength. Thus, decreasing λ and increasing NA typically results in increased spatial frequency content and in an improved, higher resolution image. The convention adopted throughout this disclosure is that spatial frequencies are given as the inverse of the corresponding length scale in the image. Therefore, a factor of 2π is necessary to convert these spatial frequencies to the magnitude of wavevectors for detailed modeling. Hereinafter, "pitch," with dimensions of nm, is used to refer to the distance between features of a periodic pattern while "period," with dimensions of nm⁻¹, is used interchangeably with spatial frequency.

Historically, the semiconductor industry has worked to both decrease λ and increase NA in its steady progress towards smaller feature sizes. There are several factors that together suggest that continued improvements to λ and NA are most likely not feasible and the industry will have to undergo a significant change in lithographic technique. Problems typically include the reduction of the feature size to below the available optical wavelengths, often decreasing the manufacturing process window, while at the same time demanding increased linewidth control for high-speed circuit operation. Moreover, for wavelengths below the 193nm ArF wavelength, transmitting optical materials are typically no longer available, forcing the need for an allreflective system. However, an all-reflective system is often problematical since current multi-layer reflector and aspheric optical technologies are typically not sufficiently developed to meet the feature size needs. The transition to reflective optics will most likely result in a significant reduction in the possible NAs, thereby reducing the benefit of shorter wavelengths. Optical sources with wavelengths shorter than 193 nm may also not provide sufficient average power for high throughput manufacturing.

Furthermore, the complexity of the masks typically increases by a factor of about four for each ultra-large scale integration (ULSI) generation (i.e. about four times as many transistors on a die). Additionally, many of the potential advances in optical lithography, often collectively know as resolution-enhancement techniques, typically lead to increased mask complexity (serifs, helper bars, and other sub-resolution features) or require a three dimensional mask in place of the traditional chrome-on-glass two-dimensional masks (phase shift techniques). The increased complexities often increase the manufacturing difficulties and costs, thereby commonly reducing the yield of the complex masks. Moreover, the transition to wavelengths shorter than 193 nm will most likely require a drastic changeover to reflective masks since transmissive optical materials with adequate optical quality are typically not available.

The limiting CD (critical dimension) of imaging optical systems is usually stated as $\kappa_1 \lambda / NA$, where κ_1 is a function



of manufacturing tolerances as well as of the optical system, λ is the center wavelength of the exposure system and NA is the numerical aperture of the imaging optical system. Typical values of κ_1 range from about 1.0 down to ~0.5. Projections for the 193 nm optical lithography tool are an NA of 0.6 which leads to a limiting CD of ~0.16 micrometer. Alternative lithographic technologies are being investigated including, inter alia, X-ray, e-beam, ion-beam and probe-tip technologies. However, none of these technologies has as yet emerged as a satisfactory alternative to optical lithography for volume manufacturing applications.

Existing nanofabrication techniques, such as e-beam lithography, have been used to demonstrate nm-scale features for a variety of applications including, inter alia, textured substrates for crystal growth, quantum structure growth and fabrication, flux pinning sites for high-T_c superconductors, form birefringent materials, reflective optical coatings, artificially created photonic bandgap materials, electronics, optical/magnetic storage media, arrays of field emitters, DRAM (Dynamic Random Access Memory) capacitors and in other applications requiring large areas of nm-scale features. However, these existing nanofabrication techniques typically remain uneconomic in that the techniques do not allow low cost manufacturing of large areas of nm-scale patterns.

In the field of textured substrates for crystal growth, 25 researchers have investigated vicinal growth (epitaxial growth on a crystal substrate polished several degrees offaxis to expose steps in the crystal faces) to provide seeding sites for growth initiation. This approach is often problematic in that the crystal steps are not well-defined and the variations lead to inhomongeneous nucleation. Moreover, in prior art epitaxial growth, the strain often limits the thickness of the film before dislocations and other defects are formed to relieve the stress.

The field of quantum structure growth and fabrication is 35 often similar to the above crystal growth application usually with the exception that the growth would involve at least two materials: a lower bandgap material typically surrounded by a higher bandgap material to provide a quantum wire or a quantum dot. Most of the current work on extremely thin 40 heterostructure materials is typically concentrated on quantum wells, 2-D planar films with thickness on the order of electronic wavefunctions (~0.1-50 nm) sandwiched in-between larger bandgap materials that form a potential barrier to confine charge carriers. These quantum well 45 materials have progressed from scientific study to important applications in high speed transistors and in optoelectronic devices such as lasers and detectors. Attempts at further reducing dimensionality from 2-D sheets to 1-D wires and 0-D boxes are often classified into three major directions: (1) 50 lithographic definition limited to ~100 nm by current techniques (primarily electron-beam lithography) and not presently scalable to large areas; (2) orientationally selective growth on wafers with large-area (um-scale) patterns which typically has significant problems with defects associated 55 with the imprecise fabrication and the three orders-ofmagnitude scale reduction required, from ~1000 nm to ~1 nm; and (3) self-assembled quantum dots usually based on modifying the growth conditions to achieve nucleation of isolated dots of material. The size and placement uniformity 60 of the dots produced by this technique is often limited by the unavoidable randomness of the nucleation and growth processes. The development of a method for uniformly defining nucleation sites by a lithographic process would have a major impact on this field.

In the field of flux pinning sites for high-T_c superconductors, allowable current densities in high tem-

perature superconductors are often limited by the motion of flux lines that induces loss and heating resulting in a phase transition to a non-superconducting state. The critical current density is the current density at which this transition occurs. An improvement potentially could be achieved by a fabrication technique that provides a predetermined density and spatial pattern of flux pinning sites by inducing localized defects in the film to trap the flux lines. In order to achieve the desired critical currents, the density of trap sites typically needs to be on the nm-scale (~5–50 nm spacings).

In the area of periodic structures, such as gratings, which play a very important role in optics, periodicities shorter than the optical wavelength could give rise to significant modifications in both the linear and nonlinear optical response of materials. For example, one-dimensional gratings with pitches much less than the wavelength can result in a birefringent response such that the reflectivity and transmission differs between light polarized along the grating and light polarized perpendicular to the grating.

Reflective optical coatings, known as Bragg reflectors, often consist of layered stacks of different materials with each layer having a 1/4-wave optical thickness. Very high reflectivities can be achieved, even with relatively small refractive index differences between the materials by using a sufficient number of layers. The extension of this concept to a periodic three dimensional optical structure is usually known as a photonic crystal. In the same way as semiconductor crystals have forbidden energy gaps within which there are no allowed electronic states, photonic crystals can exhibit photonic bandgaps where specific wavelength bands of light cannot penetrate. The ability to incorporate defects in this structure can give rise to important classes of optical emitters with unique properties such as thresholdless lasers. This new class of materials could most likely be applied to a wide range of applications.

In the electronic field, semiconductor electronics have typically been following an exponential growth in the number of transistors on a chip, increasing by a factor of four each generation (with a typical 3-year duration for each generation). As discussed above, conventional optical lithography is reaching practical limits set by available λ and NA, therefore, an advancement in lithographic techniques will be needed to manufacture these circuits.

In the field of storage media, both magnetic and optical storage densities (bits/cm²) typically have been increasing dramatically. The increased storage densities are typically a result of improvements to magnetic/optical read/write heads and to the storage media. However, traditional continuous media often allows domains to compete and grow at the expense of other domains to find the most energetically favorable configuration. Moreover, as densities continue to increase, it becomes increasingly difficult for the tracking electronics to resolve smaller distances. A cost-effective lithographic patterning technology that allows nano-scale segmentation of the storage medium potentially could address both of these issues.

Field-emitters are potentially a promising technology for cold cathode electronic devices, such as, for example, 60 mm-wave tubes and displays. These devices rely on high electric field extraction of electrons from extremely small emission areas. In the prior art, field emitter tips are typically formed by conventional lithographic definition and processing "tricks" such as shadow evaporation or three-dimensional oxidation of Si to form the nanostructures. However, the feature and current densities resulting from the prior art lower resolution lithographic techniques is not

typically sufficient for many applications. A higher resolution, nano-scale lithographic technique would have a significant impact on the development of these technologies.

In the area of DRAMs, noise considerations in readout circuitry typically require a substantially fixed capacitance for DRAM circuits independent of the total number of memory cells. Since the two-dimensional footprint available for the capacitor decreases by a factor of approximately two each DRAM generation (e.g., the 256-Mbit generation usually is scaled for a smallest printed feature (or critical 10 dimension (CD)) of 0.25 μ m and this scaling is reduced to a CD of 0.18 μ m for the 1-Gbit generation; [(0.18/0.25) 2~0.5]), simple scaling would result in an approximate factor of two reduction in the capacitance each generation. One possible approach to maintaining the needed minimum 15 capacitance is to use the third dimension by convoluting a thick capacitor structure to increase the surface area within the same two-dimensional footprint. This requires a lithographic capability beyond that required to define the circuit. However, since the industry is typically at the limits of its 20 current lithographic capability in fabricating the circuit patterns, an improved nano-scale lithographic process is required to meet these needs. Random process such as the deposition of nano-grain particles as etch masks have been demonstrated. However, the control of particle size and 25 placement is typically inadequate for a high-yield manufacturing process. Here again, development of controlled nanoscale lithography process would potentially have a significant impact.

Interferometric lithography, the use of the standing wave 30 pattern produced by two or more coherent optical beams to expose a photoresist layer, often provides a very simple technique to produce the requisite scale for the next several ULSI generations. Compared to the aforementioned problems with lithographic and non-lithographic techniques, 35 interferometric lithography typically provides a simple, inexpensive technique for defining extreme submicron array patterns over a large area without the need for a photomask. Interference effects between two coherent laser beams often have been used to create simple grating patterns in a 40 photoresist. Furthermore, interference lithography typically has a very large depth of field, so patterns can be exposed over large variations in topography. Moreover, interferometric lithography often allows very high resolution patterns to be defined on a wafer, substantially finer than those available 45 from conventional lithographic techniques, with a throughput often comparable to that of a conventional optical stepper. Therefore, a large number of structures applicable to microelectronic devices and circuits can be fabricated using interferometric lithography, either alone or in combination 50 with other lithographic techniques such as optical steppers. See U.S. Pat. No. 5,415,835—S. R. J. Brueck and Saleem Zaidi, Method and Apparatus for Fine-Line Interferometric Lithography (issued May 16, 1995); U.S. patent application Ser. No. 08/407,067—S. R. J. Brueck, Xiaolan Chen, Daniel 55 J. Devine and Saleem H. Zaidi, Methods and Apparatuses for Lithography of sparse Arrays of Sub-micrometer Features (CIP filed Mar. 13, 1995); U.S. patent application Ser. No. 08/614,991—S. R. J. Brueck, Xiaolan Chen, Daniel J. Devine and Saleem H. Zaidi, Methods and Apparatuses for 60 Lithography of sparse Arrays of sub-micrometer Features (divisional filed Mar. 13, 1996) and, which are herein incorporated by reference.

The limiting spatial frequency of interferometric lithography is $\sim \lambda/2$, where λ is the laser wavelength, and the CD 65 for 1:1 lines and spaces is $\sim \lambda/4$. In contrast to optical lithography which at I-line has a projected limit of $\kappa_x \lambda/2$

NA~0.3 μ m, interferometric lithography has a limiting resolution of ~0.09 μ m at the same wavelength. Using the 193 wavelength, the limiting resolution of interferometric lithography is ~0.05 μ m which is already better than the current projections for EUV lithography (a wavelength of 13 nm and a NA of 0.1 leading to a CD of 0.08 μ m at a κ_1 of 0.6).

One of the major challenges for interferometric lithography is developing sufficient pattern flexibility to produce useful circuit patterns. A two-beam interferometric exposure 10 produces a periodic pattern of lines and spaces over the entire field. Multiple beam (4 or 5) exposures typically produce relatively simple repeating two-dimensional patterns such as holes or posts. More complex structures can often be formed by using multiple interferometric exposures 15 as described in U.S. Pat. No. 5,415,835—S. R. J. Brueck and Saleem H. Zaidi, Method and Apparatus for Fine-Line Interferometric Lithography (filed Sep. 16, 1992; issued May 16, 1995) and in Jour. Vac. Sci. Tech. B11, 658 (1992), which are herein incorporated by reference. Additional flexibility can often be attained by combining interferometric and optical lithography as also described in the above patent. However, thus far, demonstrations have typically been limited to fairly simple examples, e.g. defining an array of lines by interferometric lithography and delimiting the field by a second optical exposure. Even with multiple exposures, more complex structures are often produced, but the overall patterns are restricted to repetitive structures.

Imaging interferometric lithography (IIL) has recently been developed [See U.S. patent application Ser. No. 08/786,066—S. R. J. Brueck, Xiaolan Chen, Andrew Frauenglass and Saleem Hussain Zaidi, Method and Apparatus for Integrating Optical and Interferometric Lithography to Produce Complex Patterns (filed Jan. 21, 1997)] as an approach to extending the spatial frequency space available for imaging, and hence allowing higher resolution images of arbitrary patterns than are usually possible with conventional optical imaging approaches. IIL is based on a linear systems approach wherein the spatial frequency space limitation of a traditional optical system is circumvented by 40 combining optical and interferometric lithographies to print regions of frequency space. Multiple exposures in the same photoresist level are then typically used to add together the different spatial frequency components to produce a final image that is significantly improved over that available with 45 traditional, single-exposure imaging optical lithography. Using this approach, it was shown that images containing spatial frequency components out to the limits of optics, $2/\lambda$, could be achieved.

As an example of the increased spatial frequency space 50 available using IIL, FIG. 1 shows a prototypical array structure that might be part of a ultra-large-scale integrated circuit, particularly a circuit with a large degree of repetitiveness such as a memory chip or a programmable logic array. The dimensional units are in terms of the critical dimension (CD-smallest resolved image dimension) which is defined in the semiconductor industry roadmap. The industry goals for the CDs are 130 nm in 2003 and 100 nm in 2006. For easy comparison, the modeling examples given herein are all for the 130-nm CD generation. The pattern consists of staggered bars each 1×2 CD². The repetitive cell is demarked by the dotted lines and is 6×6 CD². For a periodic pattern, all of the spatial frequency components are harmonics of the fundamental frequencies of this pattern, e.g. $f_x = n/L_x$; $f_y = m/L_y$, where $f_x(f_y)$ are the spatial frequencies in the x (y) direction, n (m) is an integer and $L_x=L_y=6$ CD is the repeat distance in each direction. This pattern is only introduced to illustrate the general concepts of the invention

60

65

7

and is not intended to restrict its applicability to only this or substantially similar patterns.

The goal of the lithography process is typically to reproduce this pattern in the developed resist profile with as high a fidelity as possible. FIGS. 2A and 2B show the exemplary pattern achieved when a mask with the required pattern is used in a conventional imaging optical lithography system in the limits of both incoherent (FIG. 2A) and coherent (FIG. 2B) illumination. For incoherent illumination the resultant pattern is shortened and significantly rounded appearing 10 almost circular rather than rectangular; for coherent illumination only the zero-frequency Fourier component (constant intensity across the die) is transmitted by the lens for this particular pattern, wavelength and NA combination and there is substantially no image at all. State-of-the-art lithography tools often use partially coherent illumination which is in some ways better than either of these two limits; but still shows many of the same limitations. Optics can, in principle, support spatial frequencies up to a maximum spatial frequency of $2/\lambda$. Various techniques, including multiple interferometric exposures, can almost eliminate the lens limitations on spatial frequencies and approach the fundamental limit of a linear optical system.

FIG. 3 shows the modeling results for imaging the pattern of FIG. 1 including all of the spatial frequencies available at 25 an imaging wavelength of 365 nm (I-line). While the image is significantly closer to the desired pattern than the incoherent imaging results, there is still significant rounding of the corners of the printed features due to the unavailability of the spatial frequencies needed to provide sharp corners. That is, the magnitudes of the spatial frequencies necessary to define these corners are greater than 2/λ, the limit of a linear optical system. One approach to improving upon this problem is typically to decrease the wavelength, thereby increasing the maximum available spatial frequency. Decreasing the wavelength has often been a traditional industry solution to the need for defining smaller and smaller features. However, for the reasons cited above, it is likely that this solution cannot be exploited much beyond the 193-nm ArF excimer laser source wavelength.

The use of the nonlinear response of photoresist to substantially sharpen developed photoresist patterns in the z-direction, through the thickness of the resist, has long been understood [see, for example, Introduction to Microlithography, Second Edition, L. F. Thompson, C. G. 45 Willson and M. J. Bowden, eds. (Amer. Chem. Soc. Washington D.C., 1994, pp. 174-180)]. To aid in understanding this process, many approaches exist for modeling the photoresist response. Industry-standard modeling codes, such as PROLITHTM and SAMPLE, typically take into account the many subtle effects that are often necessary to accurately model the lithography process. However, for the present purposes, a simpler model, first presented by R. Ziger and C. A. Mack [Generalized Approach toward Modeling Resist Performance, AIChE Jour. 37, 1863–1874 (1991)], typically 55 provides a good approximation. This model describes the photoresist thickness, t(E), after the photoresist develop step substantially resulting from a given optical exposure fluence (typically normalized to a clearing fluence) E by the relationship:

$$t(E) = 1 - \left(\frac{1 - e^{-E}}{1 - e^{-1}}\right)^n \tag{1}$$

where n is a parameter that characterizes the contrast of the resist. For typical novolac-based photoresist commonly used Support for "high spatial frequencies"

for I-line wavelengths, n~5–10. FIG. 4 shows a plot of t(E) vs. E showing the strong nonlinearity often associated with the photoresist process. In order to make the mathematics simpler, the modeling presented herein uses a simple thresholding step function approximation to $\tau(E)$ shown, for example, by the dotted line in FIG. 4. This approximation substantially retains the essential features of the photoresist response without introducing unnecessary computational complexity into the modeling. A more complete modeling effort can be created by one of ordinary skill in the art.

For a simple two-beam interference, the fluence profile is given by the expression:

$$E(x) = 1 + \cos(4\pi\sin(\theta)x/\lambda). \tag{2}$$

15

30

35

The Fourier transform consists of three components, a unity amplitude, zero frequency term and two components with 20 amplitude ½ at $\pm 2 \sin{(\theta)/\lambda} [F(E)=\delta(f_x)+\frac{1}{2}(\delta(f_x+2\sin{(\theta)/\lambda})+\delta(f_x-2\sin{(\theta)/\lambda}))]$, where F represents the Fourier-transform operator and f_x is the spatial frequency. After passing this function through the nonlinear filter of the photoresist, represented by $\tau(E)$, the resulting thickness of the photoresist is typically a substantially rectangular function and the Fourier transform is typically a substantially sinc (sin (x)/x) function sampled at harmonics of the pitch, $f_n=2n\sin{(\theta)/\lambda}$:

$$\tau[E(x)] = \frac{a}{2} \sum_{n=-\infty}^{\infty} \left[\frac{\sin\left(\frac{2\pi n a \sin(\theta)}{\lambda}\right)}{\frac{2\pi n a \sin(\theta)}{\lambda}} e^{i4\pi n x \frac{\sin(\theta)}{\lambda}} \right]$$
(3)

Examples of these one-dimensional real space and spatial frequency space results are shown in FIGS. 5A and 5B respectively.

FIG. 5C shows an experimental realization of this sharpening in the z-direction. This result was obtained using two coherent beams from an Ar-ion laser (λ =364 nm) incident on a photoresist-coated wafer at angles $\pm \theta$ of approximately 30° corresponding to a pitch of about 360 nm. A standard I-line photoresist was used with a thickness of about 0.5 μ m. An antireflective coating (ARC) layer was included under the photoresist to eliminate the standing wave effects that often occur as a result of the substantial reflectivity at the photoresist/Si interface. The developed photoresist features exhibit substantially vertical sidewalls. The Fourier transform of this pattern contains high spatial frequency components that go well beyond the $2/\lambda$ linear systems limit of optics as is illustrated in FIG. 5B.

While the nonlinearity often substantially sharpens the profile in the z-direction, it does not, however, usually add additional frequency components in the x-y plane. In fact, the profiles of FIGS. 2 and 3 were calculated using this same photoresist filter, thus demonstrating the lack of frequency components in the x-y plane. Moreover, multiple exposures in the same level of photoresist without any additional processing result in summing the amplitudes and phases of the spatial frequency components contained within each exposure. Consequently, applying and developing the photoresist after this summation again usually sharpens the photoresist vertical profiles but does not often substantially change the 2-D cross section at the threshold level. Mathematically, this is represented as:

$$T(x, y) = \tau \left(\sum_{n} E_{n}(x, y) \right)$$
(4)

where T(x,y) is the photoresist thickness as a function of the wafer plane Cartesian coordinates x and y and $E_n(x,y)$ is the fluence of the n^{th} exposure at the position (x,y).

A simple two exposure situation involving only two beam exposures can serve as a typical example of the prior art. The first exposure writes a periodic pattern in the x-direction as in Eq. 4, and the second exposure writes a periodic pattern at ½ the x-pitch in the y-direction. FIG. 6A shows the results of a simple double exposure, as taught in U.S. Pat. No. 5,415,835—S. R. J. Brueck and Saleem Zaidi, Method and Apparatus for Fine-Line Interferometric Lithography (issued May 16, 1995) which is herein incorporated by reference. The parameters of the calculation are set for a CD of about 130 nm and a small pitch of about 260 nm. Because the intensities are added before the thresholding operation is applied, the resulting shapes exhibit significant rounding of the comers and are substantially elliptical rather than rectangular.

SUMMARY OF THE INVENTION

The present invention extends the available spatial frequency content of an image through the use of a method and apparatus for combining nonlinear functions of intensity of at least two individual exposures to form three dimensional patterns with spatial frequencies that are not present in any of the individual exposures and that extend beyond the limits set by optical propagation of spatial frequencies whose magnitudes are $\leq 2/\lambda$ in all three spatial directions. This extension of spatial frequencies preferably extends the use of currently existing photolithography capabilities, thereby resulting in a significant economic impact. Extending the spatial frequency range of lithographically defined structures suitably allows for substantial improvements in, inter alia, crystal growth, quantum structure growth and fabrication, flux pinning sites for high-T_c superconductors, form birefringent materials, reflective optical coatings, photonic crystals, electronics, optical/magnetic storage media, arrays of field emitters, DRAM (Dynamic Random Access Memory) capacitors and in any other applications requiring large areas of nm-scale features.

A first exemplary embodiment uses two photoresist layers sensitive at different wavelengths. Additional layers are often required in a multi-level photoresist process to protect against interdiffusion of the various photosensitive materials. Alternatively, a hard mask (e.g. SiO₂ or Si₃N₄ or any other suitable film material) is used with additional processing between exposures. In either case, a first lithographic pattern at a first wavelength regime is suitably exposed into the first photosensitive layer and a second lithographic pattern in a second wavelength regime is suitably exposed into the second photosensitive layer. Upon suitable development and/or processing the result is a layering of the two lithographic patterns in the two layers and/or in the hard mask layer. These layers in combination are used as masks for further processing of the underlying wafer to transfer a 60 pattern that is the product of the two masks into the underlying materials. Image reversal offers the possibility of combining the two exposures in the same level of photoresist with intermediate processing steps to assure independent thresholding nonlinearities.

A second exemplary embodiment of combining nonlinear processes preferably includes the following steps: 1) deposit

Support for "combining nonlinear functions of intensity . . . "

Support for "combined mask . . . "

Support for "[First/Second] Pattern is

a suitable hard mask material and a photoresist layer onto the film stack to be patterned; 2) suitably expose and develop a periodic pattern (at pitch $p_{min} \ge \lambda/2$ and with CD $\le \lambda/8$) in the photoresist using interferometric lithography; 3) transfer this pattern into the hardmask by etching; 4) suitably remove the remaining photoresist; and 5) repeat the above steps at the same pitch, but with the pattern offset by $p_{min}/2$ to interpolate new features midway between the previously defined features in the hardmask. This procedure typically 10 results in a pattern with ½ the pitch of the original structure. Alternatively, this procedure may be repeated a number of times, with appropriate offsets and CDs to produce a pitch p_{min}/N , where N=1 (original pattern), N=2 (one additional exposure and processing sequence), N=3 (two additional exposures and processing sequences), and so on. Structures with linewidths as much as a factor of 40 less than the pitch for larger pitches (0.05- μ m wide line on a 2 μ m pitch) have been suitably produced [see, X. Chen et al., SPIE 1997].

In an alternative embodiment, this technique can be extended to two-dimensional patterning by using either multiple exposures and/or multiple-beam single exposures. For a grid of holes or posts with equal pitches, p₁, in both the x- and y-directions, a second exposure at the same pitch but shifted by p₁/2 in x and p₁/2 in y decreases the pitch (now p₂) to approximately p₂=p₁/√2. With two further exposures a new pitch (now p₃) of approximately p₃=p₁/2 is achieved.

BRIEF DESCRIPTION OF THE DRAWINGS FIGURES

The subject invention will be hereinafter described in conjunction with the appended drawing figures, wherein like numerals denote like elements, and:

30

FIG. 1 shows a prototypical array structure (that could be part of a memory chip or programmable logic array) having a grid in units of critical dimensions (CD) which vary for each generation and a repeating cell;

FIGS. 2A and 2B show exemplary modeling results for the two limits of incoherent (FIG. 2A) and coherent (FIG. 2B) illumination using an optical system consisting of an industry-standard I-line (365 nm) lithography tool with a 0.5 numerical aperture (NA) lens to print the pattern of FIG. 1 for a 130-nm CD;

FIG. 3 shows modeling results (I-line wavelength and 130 nm CD) using all of the spatial frequencies available to a linear optical system (to a magnitude of $2/\lambda$);

FIG. 4 shows an exemplary graph of nonlinear response of the photoresist thickness on exposure fluence with two approximations 1) the model of Ziger and Mack, t(E) with n=5 and with n=10, typical of the range of commercially available novolac resists at I-line; and 2) a simplified step function model $\tau(E)$;

FIGS. 5A and 5B show real space (FIG. 5A) and spatial frequency space (FIG. 5B) patterns for a simple two-beam interference for the aerial image and the resulting photoresist profile after the nonlinear thresholding response of the photoresist;

FIG. 5C shows an exemplary cross section scanning electron micrograph of a line:space pattern resulting from developing a two beam interference exposure that illustrates the nonlinear response of the photoresist.

FIG. 6A shows model results for the photoresist pattern created by two two-beam interferometric lithography exposures oriented at right angles to each other with the x-direction pitch ½ of that of the y-direction created by the prior art process where the two exposures are summed in a

single layer of photoresist which is subsequently developed, providing a thresholding nonlinearity that sharpens the resist sidewalls but does not modify any additional spatial frequencies in the x-y plane;

FIG. 6B shows model results for the photoresist pattern 5 created by two interferometric lithography exposures with the x-direction pitch ½ of that of the y-direction created by applying thresholding nonlinearities to each exposure individually and multiplying the thresholded images to get the final image;

FIG. 7A-7B shows an experimental demonstration of the multiplication of two masks corresponding to two thresholded images. FIG. 7A shows an exemplary result of a two-beam interferometric exposure (line:space pattern) that has been transferred to a sacrificial Si₃N₄ layer by etching after exposure and development of the first exposure. FIG. 7B shows an exemplary result after depositing a second photoresist layer, exposing this second layer with a second interferometric exposure substantially at right angles to the first exposure, and developing the second photoresist layer.

FIGS. 8A-8C show the application of the present invention to the prototypical pattern of FIG. 1 wherein FIG. 8A shows the result of a simple two-beam interferometric exposure, FIG. 8B shows the result of an incoherently illuminated imaging optical exposure (NA=0.6@365 nm) and FIG. 8C shows the result of multiplying the two images using a combined mask.

FIGS. 9A-9E show a preferred embodiment of a process, using a negative photoresist, that results in a factor of two reduction in the pitch in accordance with the present inven-

FIGS. 10A-10F show a preferred embodiment of a process, using a positive photoresist, that results in a factor of two reduction in the pitch in accordance with the present 35 invention;

FIG. 11A shows an exemplary SEM after the first etch, as demonstrated in FIG. 9C, with a pitch of approximately 260 nm in accordance with the present invention.

FIG. 11B shows exemplary results after the second etch, 40 as demonstrated in FIG. 9F, with the pitch suitably reduced to ~130 nm and the CD to ~60 nm in accordance with the present invention;

FIG. 11C shows exemplary results of an anisotropic KOH etch of 0.13-mm pitch pattern into the Si using the nitride 45 layer as a hard mask in accordance with the present inven-

FIG. 11D shows an exemplary narrow line having superior vertical sidewalls which was produced by very high spatial frequencies achieved from the nonlinearities in accordance with a preferred embodiment of the present invention.

FIG. 11E shows a concept drawing of an exemplary two color separation for a typical SRAM circuit pattern demonstrating the possibilities for using spatial frequency doubling to enhance the pattern density.

FIG. 12 shows an exemplary result of a multiple exposure technique including a 0.05-µm wide photoresist line on a 2-\mu pitch, a line:space ratio of 1:10 in accordance with a preferred embodiment of the present invention;

FIG. 13 shows an example of two-dimensional patterning with a dense array of 90-nm diameter holes defined in a photoresist layer on a 1 80-nm pitch in accordance with a preferred embodiment of the present invention;

FIG. 14 shows another example of two-dimensional patterning with a dense, hexagonal close packed pattern written

with three two-beam exposures and the wafer rotated 120° between exposures in accordance with a preferred embodiment of the present invention;

FIG. 15 shows an exemplary 2-D hole pattern written with a five-beam geometry in a single exposure in accordance with a preferred embodiment of the present invention;

FIG. 16 shows an exemplary calculation of the structures obtained with the five-beam geometry of FIG. 16 when the exposure flux is increased to form an array of posts rather than the array of holes.

DETAILED DESCRIPTION OF PREFERRED EXEMPLARY EBODIMENTS

The present invention preferably employs nonlinear processes either in the photoresist intensity response and/or in additional processing steps in order to create high spatial frequencies, beyond the optical propagation limit of 2/\(\lambda\), in a pattern produced on a suitable thin-film layer on a wafer that is used, in subsequent process steps, to transfer the structures containing the high spatial frequencies in the plane of the wafer into the underlying film structure. In a preferred embodiment, two (or more) exposures are individually subjected to thresholding nonlinearities, then the images are preferably combined (added or multiplied) resulting in a pattern containing additional spatial frequencies that are not substantially present in any of the individual images. Mathematically, the specific embodiment of multiplication is equivalent to:

$$T(x, y) = \tau[E_1(x, y)] \times \tau[E_2(x, y)] \times \dots \tau[E_n(x, y)]$$

$$= \mathcal{F}^{-1} \{ \mathcal{F}[\tau[E_1(x, y)]] \otimes \dots \mathcal{F}[\tau[E_n(x, y)]] \}$$
(4)

where the \otimes

30

40

represents a convolution operation. In like manner, the embodiment of addition is represented mathematically by:

$$T_{add}(x, y) = \tau[E_1(x, y)] + \tau[E_2(x, y)] + \dots \tau[E_n(x, y)]$$

$$= \mathcal{F}^{-1} \{ \mathcal{F}[\tau[E_1(x, y)]] + \dots \mathcal{F}[\tau[E_n(x, y)]] \}$$
(5)

The thresholding operation suitably results in high spatial frequencies in the final images; the convolution operator suitably results in a final image with spatial frequencies corresponding to substantially all possible combinations (sum and difference) of the frequencies in the individual images. In a preferred embodiment, the thresholding non-linearity results in frequency components extending beyond the capabilities of an optical system (e. g. frequencies >2/\(\lambda\). Moreover, the multiplication operation preferably extends results in components extending into parts of frequency space that are not substantially addressed by the individual exposures.

In contrast to the prior art methods which typically yield rounded comers on the structures as shown in FIG. **6A**, the present invention suitably yields the patterns shown in FIG. **6B**, namely rectangles with sharp, well-defined comers. The patterns of FIG. **6B** are preferably formed in accordance with the present invention by suitably applying the thresholding nonlinearity individually to each exposure and multiplying. Mathematically, the resulting spatial frequency transform is preferably the product of appropriate [sin $(f_x a_x)/f_x a_x$] and [sin $(f_y a_y)/f_y a_y$] functions which yields the spatial Fourier transform of the desired rectangular pattern, viz:

Support for "first mask material" Support for "combining nonlinear functions of intensity . . . " Support for "high spatial frequencies" Support for "spatial frequencies"